A Systematic Method for Gain Selection of Robust PID Control for Nonlinear Plants of Second-Order Controller Canonical Form

Pyung Hun Chang, *Member, IEEE*, and Je Hyung Jung, *Member, IEEE*

***Abstract*—A systematic method to select gains of a discrete proportional-integral-derivative (PID) controller is presented. The PID controller with the gains obtained by the proposed method can robustly control nonlinear multiple-input–multiple-output (MIMO) plants in a second-order controller canonical form, such as robot dynamics. This method has been made possible by the finding that the discrete PID control is equivalent to the discrete form of time-delay control (TDC), a robust control method for nonlinear plants with uncertainty. By using this equivalence, relationships are obtained between PID gains and parameters of TDC, which enable a systematic method for the select PID gains. In addition, based on the systematic method, a simple and effective method is proposed to tune PID gains applicable to nonlinear plants with inaccurate models. This method incorporates a set of independent tuning parameters that is far less than those for conventional methods for PID gain selection. The usefulness of the proposed methods is verified through the ease and simplicity of determining PID gains for six degrees-of-freedom (DOF) programmable universal machine for assembly (PUMA)-type robot manipulator; the effectiveness of these PID gains is confirmed by the adequate and robust performance through experimentation on the robot.**

***Index Terms*—6-degrees-of-freedom (DOF) programmable universal machine for assembly (PUMA)-type robot manipulator, discrete proportional-integral-derivative (PID) controller, discrete time control system, nonlinear plants, robust PID gains selection, robust trajectory control, time delay control (TDC), sampled data system.**

I. Introduction

TODAY, proportional-integral-derivative (PID) control is used in more than 90% of various practical control systems [1]. For example, most commercial motor drivers have a PID control law built-in. There are several reasons for the popularity of the PID control. Chief among them is that their structure is simple and easy to apply heuristically, regardless of plant dynamics; in addition, their three gains have such clear physical meanings that one can attempt to tune the gains without profound theoretical backgrounds. Moreover, an appropriate gain set tends to yield acceptable performance levels. By the term *to tune*, we mean to adjust by trial-error, whereas *to select*, we mean both *to tune* and *to determine analytically*.

Recent research trends in the PID control area are well summarized in [2]. However, that study mainly focused on chemical process control systems expressed in Laplace domain. As the characteristics of most process systems differ from those of a class of *nonlinear* plants such as robot manipulators, the results developed for process control systems cannot be directly applied to nonlinear plants. It is widely perceived that PID gains for nonlinear plants are very difficult to select on the analytical basis of closed-loop stability and performance [3], [4].

For nonlinear plants, PID control has been applied to robot manipulators as well as machines having similar dynamics to robot manipulators. The research regarding PID controllers for robot manipulators can be classified into three categories. The first is research concerning the tuning methods of PID gains through the use of intelligent control schemes such as fuzzy control [3], [5]–[7], neural-net [8], or genetic methods [9]. The second type is research that focuses on the method of PID gain selection through the use of other control schemes such as optimal controls [10]–[12] or inverse dynamics controls [4]. The third centers on the method of PID gain selection using a direct stability analysis based on the Lyapunov stability [13], [14]. The foregoing studies on PID controllers for robot manipulators tend to be theoretically complex, and tend to require exact plant models.

Owing to their complexity and the need of exact plant models, the many studies on PID control tend to be difficult for practicing engineers to fully understand and to competently apply to practical systems. Furthermore, the difficulty is compounded in applying the findings of research to many practical devices, where *tuning PID gains* is the only thing users are allowed to do.

It is no wonder that, in practice, the gains have mostly been tuned heuristically. Yet, a heuristic approach has its own problems, as there are too many gains to tune simultaneously. For example, a 6-degrees-of-freedom (DOF) robot manipulator has 18 gains—three for each joint—to be tuned, and tuning each gain requires the tunings of the rest of others owing to dynamics coupling, which in turn require the tunings of the rest, and so forth. An obvious consequence is that one never becomes convinced as to whether or not the resulting gain set is good enough. Sometimes, the Ziegler–Nichols method [15] helps; but is not always effective: it has been widely observed that the gains tuned by this method often do not yield a satisfactory performance for nonlinear plants [16].

In addition, despite that nearly every control platform currently incorporates digital devices such as microprocessors or

Manuscript received July 05, 2007; revised February 07, 2008. Manuscript received in final form April 24, 2008. First published September 30, 2008; current version published February 25, 2009. Recommended by Associate Editor L. Villani. This work was supported in part by SRC/ERC program of the Korea Science and Engineering Foundation (KOSEF) under Grant R11-1999-008 funded by the Korea government (MOST) and by Unmanned Technology Research Center (UTRC) of Agency for Defence Development under Grant UD070057AD.

P. H. Chang is with the Mechanical Engineering Department, Korea Advanced Institute of Science and Technology (KAIST), Daejeon, 305-701, Republic of Korea (e-mail: phchang@mecha.kaist.ac.kr).

J. H. Jung is with the Biorobotics Department, FATRONIK, E-20009 San Sebastián, Spain (e-mail: jhjung@fatronik.com).

Digital Object Identifier 10.1109/TCST.2008.2000989

PCs or digital signal processors (DSPs), previous research has often been formulated in a continuous time domain.

For the aforementioned reasons, we are going to propose a systematic method for the gain selection of discrete PID controllers from the viewpoint of *sampled-data* system—proposing this method is the first contribution of this article. Incidentally, by sampled-data system we mean a system having both discrete and continuous signals [17]. Using the proposed systematic method, one can determine the robust PID gains analytically when the plant model is well known. However even if the plant model is barely known, the method enables to determine the robust PID gains by simple and effective tuning—this tuning scheme is the second contribution. The idea central to the aforementioned gain-selection method is our finding that PID control is *equivalent* to time delay control (TDC) [18]–[20] a well known robust control scheme, when the plant is of the *second-order controller canonical form* and when TDC and PID controls are implemented in *discrete time domain*. This finding is the third contribution of this brief.

To briefly explain TDC, it uses the time-delayed values of control inputs and derivatives of state variables at the previous time step to cancel the nonlinear dynamics and the uncertainties such as parameter variations and disturbances. Thus, TDC does not require any real-time computations of nonlinear dynamics, nor does it use parameter estimations as an adaptive control does. As a result, TDC shows unusually robust responses under the aforementioned uncertainties; yet is simple and computationally efficient—as efficient as a PID control. Thus far, TDC has been applied to numerous real systems; such as robot systems [21]–[25], a magnetic bearing [26], a brushless DC motor [27], a robotic excavator [28], [29], a telescopic handler [30], a frictionless positioning device [31], and a PM synchronous motor [32]. In these applications, TDC has obtained satisfactory results even under large system parameter variations and disturbances.

Owing to the equivalence to TDC, the PID control with the gains determined by the aforementioned systematic method, too, is expected to possess the positive attributes of TDC, that is, robust performance and simplicity (or efficiency): it could also display adequate performance under substantial system uncertainty; and could reduce the number of PID tuning gains, far less than those for conventional methods for PID gain selection. These attributes will be confirmed both theoretically and experimentally throughout this brief.

In Section II, as preliminaries and backgrounds, the plant of our concern is presented and TDC is reviewed briefly. Section III presents a discrete PID control and a discrete TDC as well as their relationship. Section IV describes a systematic method for robust PID gain selection. Based on the systematic method, a *tuning* method of PID gains is also presented for nonlinear plants the models of which are barely known. In Section V, we apply the proposed method to tune PID gains and make experiments on a six-DOF programmable universal machine for assembly (PUMA)-type robot manipulator whose dynamics is *barely known*. In this case, we attempted to verify the simplicity and effectiveness of the proposed method. Finally, Section VI summarizes the results and draw conclusions.

II. Preliminaries and Backgrounds

In this section, as preliminaries, we are going to briefly present the plant of our concern, and TDC to the extent that is necessary to investigate the relationship with the PID control. A more complete coverage of TDC will be found in [18]–[21].

A. Object Plant

An object plant is a nonlinear multiple-input–multiple-output (MIMO) plant in *second-order controller canonical form* or phase variable form described as follows:

$$\ddot{\mathbf{x}} = \mathbf{f}(\mathbf{x}, \dot{\mathbf{x}}) + \mathbf{g}(\mathbf{x}, \dot{\mathbf{x}})\mathbf{u}. \tag{1}$$

Here, $\mathbf{x} \in \Re^n$ denotes the state vector to be controlled, $\mathbf{u} \in \Re^n$ the input vector, $\mathbf{f} \in \Re^n$ an unknown nonlinear vector function including unmodelled terms such as frictions and disturbances, and $\mathbf{g} \in \Re^{n \times n}$ denotes an input distribution matrix.

B. Time Delay Control

In this brief, TDC referred to in [19] is used. To derive TDC for (1), an error vector is defined as

$$\mathbf{e} = \mathbf{x}_d - \mathbf{x} \tag{2}$$

where $\mathbf{x}_d$ denotes the desired output vector. If $\mathbf{g}^{-1}$ exists, the application of control input

$$\mathbf{u} = \mathbf{g}(\mathbf{x}, \dot{\mathbf{x}})^{-1}(-\mathbf{f}(\mathbf{x}, \dot{\mathbf{x}}) + \mathbf{v}) \tag{3}$$

to the plant (1) leads to the cancellation of the nonlinearities, resulting in a *decoupled* input–output relation

$$\ddot{\mathbf{x}} = \mathbf{v} \tag{4}$$

where $\mathbf{v}$ denotes a new input vector. For tasks involving the tracking of a desired output vector $\mathbf{x}_d$, $\mathbf{v}$ is selected as

$$\mathbf{v} = \ddot{\mathbf{x}}_d + \mathbf{k}_D\dot{\mathbf{e}} + \mathbf{k}_P\mathbf{e} \tag{5}$$

with $\mathbf{k}_D$ and $\mathbf{k}_P$ being $n \times n$ constant diagonal matrices, whose ith diagonal elements k_{D_i} and k_{P_i}, respectively, are chosen so that the polynomials

$$p^2 + k_{D\_i}p + k_{P\_i}(\text{for } i = 1, \cdots, n) \tag{6}$$

may become Hurwitz. This leads to an exponentially stable and decoupled error dynamics

$$\ddot{\mathbf{e}} + \mathbf{k}_D\dot{\mathbf{e}} + \mathbf{k}_P\mathbf{e} = 0 \tag{7}$$

which implies that the error vector $\mathbf{e}(t)$ converges to zero vector $(\mathbf{e}(t) \to \mathbf{0})$.

In practice, however, it is impossible to know the exact models of $\mathbf{f}(\mathbf{x}, \dot{\mathbf{x}})$ and $\mathbf{g}(\mathbf{x}, \dot{\mathbf{x}})$. Therefore, it becomes desirable to design a control law that cancels the nonlinear dynamics like

(3) does, even when the exact models of $\mathbf{f}(\mathbf{x},\dot{\mathbf{x}})$ and $\mathbf{g}(\mathbf{x},\dot{\mathbf{x}})$ are not known. To this end (1) is rearranged into the following:

$$\ddot{\mathbf{x}} = \mathbf{H} + \bar{\mathbf{g}}u \tag{8}$$

where $\bar{\mathbf{g}}$ denotes a constant diagonal matrix with non-zero element and $\mathbf{H}$ consists of all the terms representing uncertainties, expressed as

$$\mathbf{H} = \mathbf{f}(\mathbf{x},\dot{\mathbf{x}}) + (\mathbf{g}(\mathbf{x},\dot{\mathbf{x}}) - \bar{\mathbf{g}})\mathbf{u}. \tag{9}$$

Set the control law as

$$\mathbf{u} = \bar{\mathbf{g}}^{-1}(-\bar{\mathbf{H}} + \mathbf{v}) \tag{10}$$

where $\bar{\mathbf{H}}$ denotes an *estimation of* $\mathbf{H}$. Note that, if $\bar{\mathbf{H}} = \mathbf{H}$, (10) is equivalent to (3), that is, simply another expression of (3).

Instead of trying to achieve $\bar{\mathbf{H}} = \mathbf{H}$, TDC uses the following estimation scheme. If $\mathbf{f}(\mathbf{x},\dot{\mathbf{x}})$ is continuous, and time delay λ is *sufficiently* small so that $\mathbf{f}(\mathbf{x},\dot{\mathbf{x}})$ does not vary significantly during λ, then the following approximation holds:

$$\boldsymbol{\epsilon}(t) \triangleq \mathbf{H}(t-\lambda) - \mathbf{H}(t) \cong \mathbf{0}. \tag{11}$$

This relationship is used together with (8) to obtain what is called *time-delay estimation* (TDE) as the following:

$$\bar{\mathbf{H}} = \mathbf{H}(t-\lambda) = \ddot{\mathbf{x}}(t-\lambda) - \bar{\mathbf{g}} \cdot \mathbf{u}(t-\lambda). \tag{12}$$

In addition, $\boldsymbol{\epsilon}(t)$ in (11) is termed *TDE error* at t. Combining (5) and (10) with (12), TDC is obtained as

$$\mathbf{u}(t) = \mathbf{u}(t-\lambda) + \bar{\mathbf{g}}^{-1}(-\ddot{\mathbf{x}}(t-\lambda) + \ddot{\mathbf{x}}_d + \mathbf{k}_D\dot{\mathbf{e}} + \mathbf{k}_P\mathbf{e}). \tag{13}$$

Note that $\mathbf{k}_D, \mathbf{k}_P$, and $\bar{\mathbf{g}}$ determine the performance and stability of TDC. In previous research works [18]–[23], $\bar{\mathbf{g}}$ has been selected in two different manners as the following.

- Type I: $\bar{\mathbf{g}} = \bar{g}_c \cdot \mathbf{I}_n$, where $\bar{g}_c$ denotes a constant and $\mathbf{I}_n$ denotes a $n \times n$ identity matrix. That is, all diagonal elements of $\bar{\mathbf{g}}$ are identical to $\bar{g}_c$.
- Type II: Diagonal matrix with different diagonal values ($(\bar{\mathbf{g}})_{\text{ii}} = \bar{g}_i$ for $i = 1, \ldots, n$).

Remark 1: As shown in (13), since TDC does not use the knowledge of $\mathbf{f}(\mathbf{x},\dot{\mathbf{x}})$ and $\mathbf{g}(\mathbf{x},\dot{\mathbf{x}})$, it is robust for systems with poorly known dynamics. In many previous works [18]–[32], this fact is well shown by means of analysis, simulations, and experiments.

Remark 2: Due to the approximation of (11), if the discontinuous uncertainties are included in $\mathbf{H}(t)$, they cause a considerable estimation error in discontinuous region. This phenomenon and the remedies for that are well presented in [29], [34], and [35].

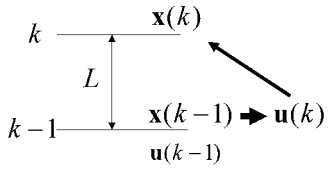

Fig. 1. Causality relationship between $\mathbf{x}$ and $\mathbf{u}$ in the discrete time control system.

III. Relationship Between Discrete TDC and Discrete PID Controller

In discrete time control systems, the control input is implemented with digital devices such as microprocessors or PCs according to causality relationship between $\mathbf{x}$ and $\mathbf{u}$—the relationship specifying which variable is independent, and which dependent. Fig. 1 illustrates the relationship: $\mathbf{u}(k-1)$ and $\mathbf{x}(k-1)$ determines (or causes) $\mathbf{u}(k)$, which together with $\mathbf{x}(k-1)$ determines $\mathbf{x}(k)$. Here, k denotes the time at the kth sampling instant t_k, that is, $t_k = Lk$, with L being the sampling period.

A. Discrete Time Delay Control

1) Discrete TDC Law: Although (13) is in continuous form, TDC law is usually implemented in digital devices. Considering that λ in (13) needs to be sufficiently small and that the smallest λ one can achieve in digital devices is the sampling period L, one may express (13) in a discrete form as

$$\mathbf{u}(k) = \mathbf{u}(k-1) + \bar{\mathbf{g}}^{-1}(-\ddot{\mathbf{x}}(k-1) + \ddot{\mathbf{x}}_d(k-1) + \mathbf{k}_D\dot{\mathbf{e}}(k-1) + \mathbf{k}_P\mathbf{e}(k-1)). \tag{14}$$

In deriving (14) from (13), the causality relationship mentioned before has made it necessary to transform $\ddot{\mathbf{x}}_d(t), \dot{\mathbf{e}}(t), \mathbf{e}(t)$ to $\ddot{\mathbf{x}}_d(k-1), \dot{\mathbf{e}}(k-1), \mathbf{e}(k-1)$ instead of $\ddot{\mathbf{x}}_d(k), \dot{\mathbf{e}}(k), \mathbf{e}(k)$.

In addition, owing to the limited availability of sensors, $\ddot{\mathbf{x}}$ and $\dot{\mathbf{x}}$ are usually obtained by numerical differentiation, as follows:

$$\dot{\mathbf{x}}(k) = \frac{\mathbf{x}(k) - \mathbf{x}(k-1)}{L}$$
$$\ddot{\mathbf{x}}(k) = \frac{\mathbf{x}(k) - 2\mathbf{x}(k-1) + \mathbf{x}(k-2)}{L^2}. \tag{15}$$

If $\ddot{\mathbf{x}}_d$ and $\dot{\mathbf{x}}_d$ are also obtained by numerical differentiation as in (15), (14) is rewritten as

$$\mathbf{u}(k) = \mathbf{u}(k-1) + \bar{\mathbf{g}}^{-1}\left(\frac{\mathbf{e}(k-1) - 2\mathbf{e}(k-2) + \mathbf{e}(k-3)}{L^2} + \mathbf{k}_D\frac{\mathbf{e}(k-1) - \mathbf{e}(k-2)}{L} + \mathbf{k}_P\mathbf{e}(k-1)\right). \tag{16}$$

Note that (16) represents the discrete TDC that will be used.

2) Stability of Discrete Time Delay Control: Owing to the finite time delay one can achieve in digital devices, there exists

the TDE error defined in (11), and as the result of [33], the error dynamics (7) can be transformed as

$$\ddot{\mathbf{e}}(t) + \mathbf{k}_D\dot{\mathbf{e}}(t) + \mathbf{k}_P\mathbf{e}(t) = \boldsymbol{\epsilon}(t). \tag{17}$$

Under the assumption of $\mathbf{x}_d, \dot{\mathbf{x}}_d, \ddot{\mathbf{x}}_d \in L_2^n$, where L_2^n is defined as the set of all piece-wise continuous functions $\mathbf{h} : [0, \infty) \to \Re^n$, such that

$$\|\mathbf{h}\|_{L_2} = \sqrt{\int_0^\infty \mathbf{h}^T(t) \cdot \mathbf{h}(t)dt} < 0 \tag{18}$$

a sufficient condition for closed-loop stability under discrete TDC is presented in [33] as the following:

$$\|\mathbf{I}_n - \mathbf{g}(\mathbf{x}, \dot{\mathbf{x}}) \cdot \bar{\mathbf{g}}^{-1}\|_{i2} < \frac{1}{1 + [(1 + \beta_1\gamma_P)\gamma_D + \beta_2\gamma_{\mathrm{PD}}]L} \tag{19}$$

where the subscript $i2$ denotes the induced matrix *two*-norm, and

$$\gamma_D = \|\mathbf{k}_D\|_{i2}, \quad \gamma_P = \|\mathbf{k}_P\|_{i2}, \quad \gamma_{\mathrm{PD}} = \|\mathbf{k}_P - \mathbf{k}_D^2\|_{i2}. \tag{20}$$

In addition, β_1 and β_2 denote the L_2 gains defined as

$$\beta_1 = \|\mathbf{Q}\|_{i2}, \beta_2 = \|\mathbf{R}\|_{i2} \tag{21}$$

where $\mathbf{Q}$ denotes a diagonal matrix with the ith diagonal term as $(\mathbf{Q})_{\mathrm{ii}} = \max_\omega |q_i(j\omega)|$ and $\mathbf{R}$ a diagonal matrix with the ith diagonal term as $(\mathbf{R})_{\mathrm{ii}} = \max_\omega |r_i(j\omega)|$, with transfer functions q_i and r_i defined by

$$q_i(s) = \frac{e_i(s)}{\epsilon_i(s)} = \frac{1}{s^2 + k_{D\_i}s + k_{P\_i}} \tag{22}$$

$$r_i(s) = \frac{\dot{e}_i(s)}{\epsilon_i(s)} = \frac{s}{s^2 + k_{D\_i}s + k_{P\_i}} \tag{23}$$

where e_i denotes the ith element of $\mathbf{e}$, $\dot{e}_i$ the ith element of $\dot{\mathbf{e}}$, and ϵ_i the ith element of $\boldsymbol{\epsilon}$ of (17).

B. Discrete PID Controller

For plant (1), the PID control is expressed in a continuous time domain as

$$\mathbf{u}(t) = \mathbf{K}\left(\mathbf{e}(t) + \mathbf{T}_D\dot{\mathbf{e}}(t) + \mathbf{T}_I^{-1}\int_0^t \mathbf{e}(\sigma)d\sigma\right) + \mathbf{u}_{\mathrm{DC}} \tag{24}$$

where $\mathbf{K}$ denotes a $n \times n$ constant diagonal proportional gain matrix, $\mathbf{T}_D$ a $n \times n$ constant diagonal matrix representing derivative time, $\mathbf{T}_I$ a $n \times n$ constant diagonal matrix representing a reset or integral time, and $\mathbf{u}_{\mathrm{DC}}$ denotes a $n \times 1$ constant vector representing a dc-bias decided by initial conditions. Clearly, the number of PID gains is $3n$ except for $\mathbf{u}_{\mathrm{DC}}$.

When a PID control is implemented in digital devices, by the causal consideration, (24) can be obtained in discrete form as

$$\mathbf{u}(k) = \mathbf{K}\left(\mathbf{e}(k-1) + \mathbf{T}_D\dot{\mathbf{e}}(k-1) + \mathbf{T}_I^{-1}\sum_{i=0}^{k-1} L \cdot \mathbf{e}(i)\right) + \mathbf{u}_{\mathrm{DC}}. \tag{25}$$

It is possible to transform (25) into another form by the following procedures.

First, obtain $\mathbf{u}(k-1)$ for $k \geq 2$ by using (25) and subtract it from $\mathbf{u}(k)$ in (25), then results the following relationship:

$$\begin{aligned}\mathbf{u}(k) - \mathbf{u}(k-1) = \mathbf{K}((\mathbf{e}(k-1) - \mathbf{e}(k-2)) \\ + \mathbf{T}_D(\dot{\mathbf{e}}(k-1) - \dot{\mathbf{e}}(k-2)) + \mathbf{T}_I^{-1} \cdot L \cdot \mathbf{e}(k-1)).\end{aligned} \tag{26}$$

Second, use (15) to obtain $\dot{\mathbf{x}}$ and $\dot{\mathbf{x}}_d$ in order to determine $\dot{\mathbf{e}}(\cdot)$ terms in (26). Rearranging it leads to

$$\begin{aligned}\mathbf{u}(k) = \mathbf{u}(k-1) + \mathbf{K} \cdot L \\ \cdot \left(\mathbf{T}_D\frac{\mathbf{e}(k-1) - 2\mathbf{e}(k-2) + \mathbf{e}(k-3)}{L^2}\right. \\ \left. + \frac{\mathbf{e}(k-1) - \mathbf{e}(k-2)}{L} + \mathbf{T}_I^{-1}\mathbf{e}(k-1)\right)\end{aligned} \tag{27}$$

for $k \geq 2$. Note that (27) is the result for discrete PID controller which is to be compared with the discrete TDC.

C. Relationship Between Discrete TDC and Discrete PID Controller

The relationship between discrete TDC and discrete PID controller is established in the following Theorem 1.

Theorem 1: Consider the nonlinear plant (1), discrete TDC (14), and discrete PID control (25). If the following hold:

a) first and second differentiation of output $\mathbf{x}$ and desired output $\mathbf{x}_d$ for time are obtained by numerical differentiation of $\mathbf{x}$ and $\mathbf{x}_d$ like (15);
b) $(\mathbf{K}, \mathbf{T}_D, \mathbf{T}_I)$ of the PID control has the relationship to $(\bar{\mathbf{g}}, \mathbf{k}_D, \mathbf{k}_P)$ of TDC as:
   Relationship 1: $\mathbf{K} = (\bar{\mathbf{g}}^{-1}\mathbf{k}_D)/(L), \mathbf{T}_D = \mathbf{k}_D^{-1}, \mathbf{T}_I = \mathbf{k}_D\mathbf{k}_P^{-1}$.
c) $\mathbf{u}_{\mathrm{DC}}$ of PID control (25) is determined by

$$\mathbf{u}_{\mathrm{DC}} = \bar{\mathbf{g}}^{-1}[(\ddot{\mathbf{e}}(0) + \mathbf{k}_D\dot{\mathbf{e}}(0)) - L^{-1}(\dot{\mathbf{e}}(0) + \mathbf{k}_D\mathbf{e}(0))] \tag{28}$$

where $\ddot{\mathbf{e}}(0), \dot{\mathbf{e}}(0)$, and $\mathbf{e}(0)$ denote the initial values of $\ddot{\mathbf{e}}(k), \dot{\mathbf{e}}(k)$, and $\mathbf{e}(k)$, then discrete TDC (14) is equivalent with the discrete PID control (25).

Proof: Comparing (16) with (27) makes it clear that (14) and (25) are equivalent to each other and hence yields the relationship between $(\bar{\mathbf{g}}, \mathbf{k}_D, \mathbf{k}_P)$ of TDC and $(\mathbf{K}, \mathbf{T}_D, \mathbf{T}_I)$ of the PID control as Relationship 1 for $k \geq 2$. To show equivalence between (14) and (25) at $k = 1$, the condition (c) is required. This part is described as follows.

When $k = 1$, the discrete TDC (14) and discrete PID control (25) are expressed, respectively, as

$$\mathbf{u}(1)_{\text{PID\_Control}} = \mathbf{K}\left(\mathbf{e}(0) + \mathbf{T}_D\dot{\mathbf{e}}(0) + \mathbf{T}_I^{-1}\sum_{i=0}^{0} L\cdot\mathbf{e}(i)\right) + \mathbf{u}_{\text{DC}} \quad (29)$$

$$\mathbf{u}(1)_{\mathbf{TDC}} = \mathbf{u}(0) + \bar{\mathbf{g}}^{-1}\left(-\ddot{\mathbf{x}}(0) + \ddot{\mathbf{x}}_d(0) + \mathbf{k}_D\dot{\mathbf{e}}(0) + \mathbf{k}_P\mathbf{e}(0)\right) \quad (30)$$

where $\mathbf{u}(0)$ denotes the initial TDC input which is generally set to zero vector ($\mathbf{u}(0) = \mathbf{0}$). To guarantee the equivalence between the discrete TDC and discrete PID control at $k = 1$, (29) should be equal to (30), that is

$$\mathbf{u}(0) + \bar{\mathbf{g}}^{-1}\cdot(\ddot{\mathbf{e}}(0) + \mathbf{k}_D\dot{\mathbf{e}}(0) + \mathbf{k}_P\mathbf{e}(0)) = \mathbf{K}\cdot\left(\mathbf{e}(0) + \mathbf{T}_D\dot{\mathbf{e}}(0) + \mathbf{T}_I^{-1}L\mathbf{e}(0)\right) + \mathbf{u}_{\text{DC}}. \quad (31)$$

By substituting Relationship 1 into (31) and rearranging it, under the assumption that $\mathbf{u}(0) = \mathbf{0}, \mathbf{u}_{\text{DC}}$ is derived as

$$\begin{aligned}\mathbf{u}_{\text{DC}} &= \bar{\mathbf{g}}^{-1}(\ddot{\mathbf{e}}(0) + \mathbf{k}_D\dot{\mathbf{e}}(0) + \mathbf{k}_P\mathbf{e}(0)) \\ &\quad - \frac{\bar{\mathbf{g}}^{-1}\mathbf{k}_D}{L}\cdot\left(\mathbf{e}(0) + \mathbf{k}_D^{-1}\dot{\mathbf{e}}(0) + \mathbf{k}_P\mathbf{k}_D^{-1}L\mathbf{e}(0)\right) \\ &= \bar{\mathbf{g}}^{-1}\left(\ddot{\mathbf{e}}(0) + \mathbf{k}_D\dot{\mathbf{e}}(0) + \mathbf{k}_P\mathbf{e}(0)\right. \\ &\qquad \left. - \frac{\mathbf{k}_D}{L}\mathbf{e}(0) - \frac{1}{L}\dot{\mathbf{e}}(0) - \mathbf{k}_P\mathbf{e}(0)\right) \\ &= \bar{\mathbf{g}}^{-1}[\ddot{\mathbf{e}}(0) + \mathbf{k}_D\dot{\mathbf{e}}(0) - L^{-1}(\dot{\mathbf{e}}(0) + \mathbf{k}_D\mathbf{e}(0))]. \end{aligned} \quad (32)$$

The right-hand side of last term in (32) is the same as that of (28). Finally, $\mathbf{u}_{\text{DC}}$ of (25) is determined by (28), the discrete TDC and the discrete PID control become identical at $k = 1$.

Therefore, if conditions (a)–(c) are satisfied, (14) is equivalent with (25) for $k \geq 1$. ■

Since the two controls are identical, it is logical to conclude that the discrete PID control possesses the same properties as the discrete TDC such as simplicity and robust performance, which will be confirmed by experiments.

IV. Systematic Method For Gain Selection of PID Controller

On the basis of Theorem 1, the PID gains $(\mathbf{K}, \mathbf{T}_D, \mathbf{T}_I)$, and $\mathbf{u}_{\text{DC}}$ can be selected systematically. In their selections, notice that there are *two different ways* depending the availability of $\mathbf{g}(\mathbf{x}, \dot{\mathbf{x}})$: when it is available, the gains are determined analytically; if unavailable, the gains are determined by *tuning* $\bar{\mathbf{g}}$, that is, adjusting by trial and error. It is widely recognized that $\mathbf{g}(\mathbf{x}, \dot{\mathbf{x}})$ for robot manipulators—the inverse of inertia matrix—is very difficult to estimate [36]. The procedure of selecting PID gains $(\mathbf{K}, \mathbf{T}_D, \mathbf{T}_I)$ is described as follows.

Step 1) Select a sampling period L as small as possible, considering the CPU power of the digital devices; some commercial devices, however, have sampling periods already set in the factory.

Step 2) Specify $\mathbf{k}_D$ and $\mathbf{k}_p$ in (17) by considering desired closed-loop eigenvalues.

Fig. 2. Six-DOF PUMA-type robot manipulator (Faraman AC2): (a) without payload; (b) with 4.4-kg payload.

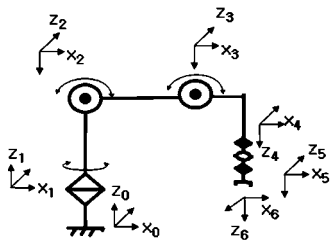

i	α_{i-1}	a_{i-1}	d_i	Θ_{i-1}
1	0	0	0	Θ_1
2	-90°	0	0	Θ_2
3	0	0.42m	0	Θ_3
4	-90°	0.1m	0.5m	Θ_4
5	90°	0	0	Θ_5
6	-90°	0	0	Θ_6

Fig. 3. D-H parameters of Faraman AC2. The robot is of a PUMA type robot having 6 DOF.

Step 3) By using $\mathbf{k}_D$ and $\mathbf{k}_P$, obtain $\mathbf{T}_I$ and $\mathbf{T}_D$ by Relationship 1. $\mathbf{K}$ too can be calculated by Relationship 1, but we need to determine $\bar{\mathbf{g}}$ first. The selection of $\bar{\mathbf{g}}$ is done either analytically or heuristically (by tuning) depending on the availability of $\mathbf{g}(\mathbf{x}, \dot{\mathbf{x}})$ as follows.

1) When $\mathbf{g}(\mathbf{x}, \dot{\mathbf{x}})$ is well known, determine first the right-hand side of (19) by calculating β_1, β_2 by (21) and $\gamma_D, \gamma_P, \gamma_{\text{PD}}$ by (20), and then analytically select $\bar{\mathbf{g}}$ satisfying (19).

2) When $\mathbf{g}(\mathbf{x}, \dot{\mathbf{x}})$ is unavailable, it becomes necessary to *tune* $\bar{\mathbf{g}}$—either $\bar{g}_c$ for Type I or $\bar{g}_i (i = 1, \ldots, n)$ for Type II. The tuning is to be done by gradually increasing from a small value until satisfactory performance is obtained. This tuning procedure is exemplified by the experiment in Section V.

Using $\bar{\mathbf{g}}$, whether analytically selected or tuned, one can also determine $\mathbf{u}_{\text{DC}}$ by (28), completing the gain selection procedure.

Associated with the previous procedure as well as measurement noise and TDE error ϵ, there are the following remarks to be made.

1) In Step 2), when the desired error dynamics is specified by the designer in terms of natural frequencies vector $\boldsymbol{\omega}_n$ and

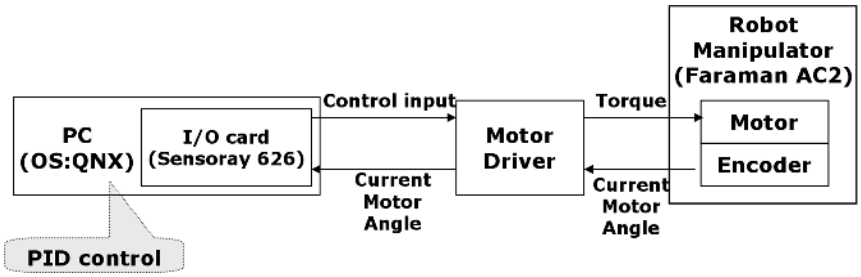

Fig. 4. Hardware structure of the control system.

damping ratios vector $\boldsymbol{\zeta}$, they are readily determined by the following relationships:

$$k_{D\_i} = 2\zeta_i \omega_{n\_i}, \quad k_{P\_i} = \omega_{n\_i}^2 \tag{33}$$

where k_{D_i} denotes the ith diagonal element of $\mathbf{k}_D$, k_{P_i} the ith diagonal element of $\mathbf{k}_P$, ω_{n_i} the ith element of $\boldsymbol{\omega}_n$ and ζ_i the ith element of $\boldsymbol{\zeta}$.

2) In our gain selection method, of the PID gains $(\mathbf{K}, \mathbf{T}_D, \mathbf{T}_I)$, $\mathbf{T}_I$, and $\mathbf{T}_D$ are determined directly by *design specifications*, for $\mathbf{T}_D = \mathbf{k}_D^{-1}$ and $\mathbf{T}_I = \mathbf{k}_D \mathbf{k}_P^{-1}$ by Relationship 1, and $\mathbf{k}_D, \mathbf{k}_P$, are to be specified when error dynamics is defined. This property is significant in the following two respects.
   (2.1) Since $\mathbf{T}_I$ and $\mathbf{T}_D$ are specified by designers, they are automatically determined at the very beginning of Step 3), leaving only $\mathbf{K}$ to be determined—through the selection of $\bar{\mathbf{g}}$ either by analytical computation or tuning as described in Step 3). Even in the case of tuning, the number of tuning parameters is either one for Type I $(\bar{g}_c)$, or two and no more than n for Type II ($\bar{g}_i$ for $i = 1, \ldots, n$). For a 6-DOF PUMA-type robot, for instance, the proposed method requires to tune either $\bar{g}_c$, or two $\bar{g}_i's$: $\bar{g}_1$ for the arm part (joints 1–3) and $\bar{g}_2$ for the wrist part (joints 4–6). By contrast, conventional methods necessitate to tune 18 gains—$\mathbf{K}, \mathbf{T}_D$, and $\mathbf{T}_I$ for 6 joints.
   (2.2) Since $\mathbf{k}_D$ and $\mathbf{k}_P$ are specified to *define error dynamics* in TDC, whereas $\bar{\mathbf{g}}$ is selected on different basis, determination of $\mathbf{k}_D$ and $\mathbf{k}_P$ are *decoupled* from that of $\bar{\mathbf{g}}$, and vice versa. That is, we can determine $\mathbf{k}_D, \mathbf{k}_P$ without regard to $\bar{\mathbf{g}}$, and $\bar{\mathbf{g}}$ regardless of $\mathbf{k}_D, \mathbf{k}_P$; furthermore, specifying $\mathbf{k}_D$ and $\mathbf{k}_P$ does not necessitate subsequent adjustments of $\bar{\mathbf{g}}$, and selecting $\bar{\mathbf{g}}$ does not require to adjust $\mathbf{k}_D$ and $\mathbf{k}_P$. In contrast, the tuning of a conventional PID gain demands the adjustment of other gains, which in turn requires further tunings of the rest of other gains, and so on.
3) In TDC, the purpose of replacing $\mathbf{g}(\mathbf{x}, \dot{\mathbf{x}})$ with a constant diagonal matrix $\bar{\mathbf{g}}$ in (8) is to cancel the off-diagonal residue $(\mathbf{g}(\mathbf{x}, \dot{\mathbf{x}}) - \bar{\mathbf{g}})\mathbf{u}$ in (9) with time-delay estimation in (12). As a result, TDC in (13) has a decoupled form without any off-diagonal term and the intended closed-loop dynamics, (4), is also decoupled. Hence, selection of $\bar{g}_i$ is meant to be *decoupled*: $\bar{g}_i$ is tuned independently without regard to $\bar{g}_j (j \neq i)$, and vice versa. Thus, $\bar{\mathbf{g}}$ can be selected without regard to $\mathbf{k}_D$ and $\mathbf{k}_P$ according to aforementioned remark (2.2) and a component of $\bar{\mathbf{g}}$ itself may be selected without regard to its other components.
4) It is interesting to observe in Relationship 1 how $\mathbf{K}, \mathbf{T}_D$, and $\mathbf{T}_I$ are related to one another. Tuning $\mathbf{K}, \mathbf{T}_D$, and $\mathbf{T}_I$ without knowing the relationship would make it almost impossible to achieve a decoupled tuning. Fortunately, however, the proposed method first determines $\mathbf{k}_D, \mathbf{k}_P$, and $\bar{\mathbf{g}}$ in a decoupled manner, and then determine $\mathbf{K}, \mathbf{T}_D$, and $\mathbf{T}_I$ by Relationship 1.
5) Remedy for measurement noise—Since TDC (14) requires the first and second derivative signals of output of system, the effect and remedy of measurement noise have been well reported in several previous TDC papers [18]–[20], [22]. In many real applications of TDC, in order to smooth out high frequency noise, the low-pass filter has been used with TDC as follows:

$$\mathbf{u}'(k) = \mathbf{u}(k-1) + \bar{\mathbf{g}}^{-1} \left(\frac{\mathbf{e}(k-1) - 2\mathbf{e}(k-2) + \mathbf{e}(k-3)}{L^2} + \mathbf{k}_D \frac{\mathbf{e}(k-1) - \mathbf{e}(k-2)}{L} + \mathbf{k}_P \mathbf{e}(k-1) \right) \tag{34}$$

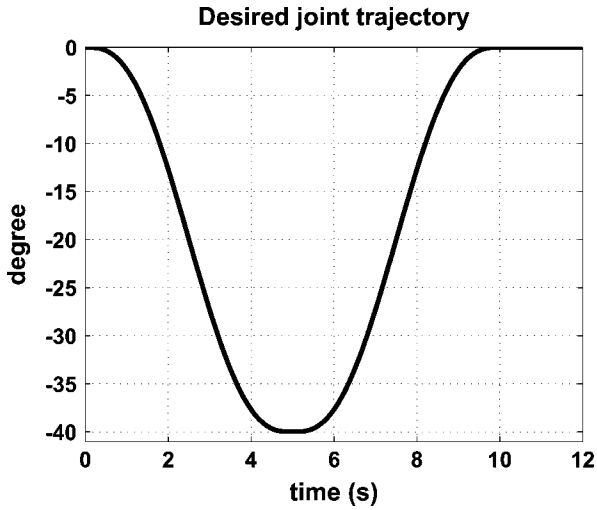

Fig. 5. Desired joint trajectory for each joint made by a fifth polynomial trajectory.

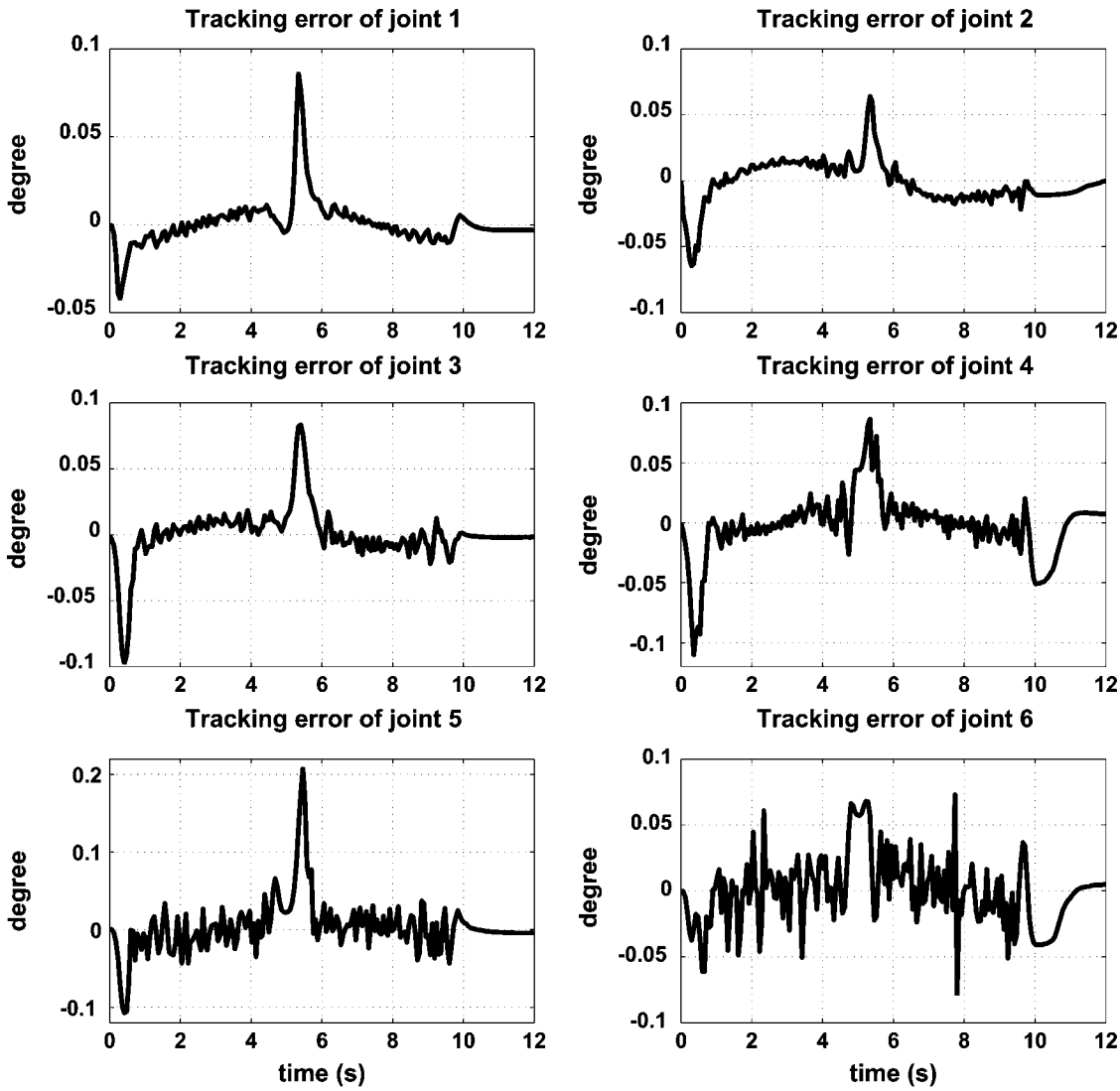

Fig. 6. Experimental results of Faraman AC2 without payload under the PID control by the proposed method. Joints 1–3 have the same PID gains and joints 4–6 same PID gains.

where $\mathbf{u}'(k)$ denotes the input to the filter and $\mathbf{u}(k)$ the output filter, i.e.,

$$\mathbf{u}(k) = \frac{\omega \cdot L}{1+\omega \cdot L}\mathbf{u}'(k) + \frac{1}{1+\omega \cdot L}\mathbf{u}(k-1) \qquad (35)$$

where ω denotes a cut-off frequency and L a sampling period. Substituting (34) into (35), $\mathbf{u}(k)$ is obtained by

$$\mathbf{u}(k) = \mathbf{u}(k-1) + \frac{\omega \cdot L}{1+\omega \cdot L}\bar{\mathbf{g}}^{-1} \times \left(\frac{\mathbf{e}(k-1) - 2\mathbf{e}(k-2) + \mathbf{e}(k-3)}{L^2} + \mathbf{k}_D \frac{\mathbf{e}(k-1) - \mathbf{e}(k-2)}{L} + \mathbf{k}_P \mathbf{e}(k-1) \right). \qquad (36)$$

Therefore, Relationship 1 is changed by the following.

Relationship 2: $\mathbf{K} = \omega \bar{\mathbf{g}}^{-1}\mathbf{k}_D/(1+\omega L), \mathbf{T}_D = \mathbf{k}_D^{-1}, \mathbf{T}_I = \mathbf{k}_D\mathbf{k}_P^{-1}$.

From Relationship 2, in order to smooth out high frequency measurement noise, the proportional gain matrix $\mathbf{K}$ must be smaller than the case without the output measurement noise. This is well-know fact like Remark 7 in [4].

6) Effect of TDE error $\boldsymbol{\epsilon}$: $\boldsymbol{\epsilon}$ given by (11) increases with the following two cases:

Case 1) when the discontinuous uncertainties are included in a system dynamics (Remark 2);

Case 2) when time delay (sampling period L) increases.

Since our approach is based on equivalent relationship between TDC and PID controller in discrete-time domain, PID controller with the gains obtained by our method has the same weak point as TDC under Case 1). By equivalence with TDC, we can guess that this problem can be solved similarly to the case of TDC [29], [34], [35]. However, since this topic deviates from main objective of this brief, we will deal with this matter as further research work. In relation to Case 2), it is well-known fact that the selection of sampling period L needs to be based on the higher

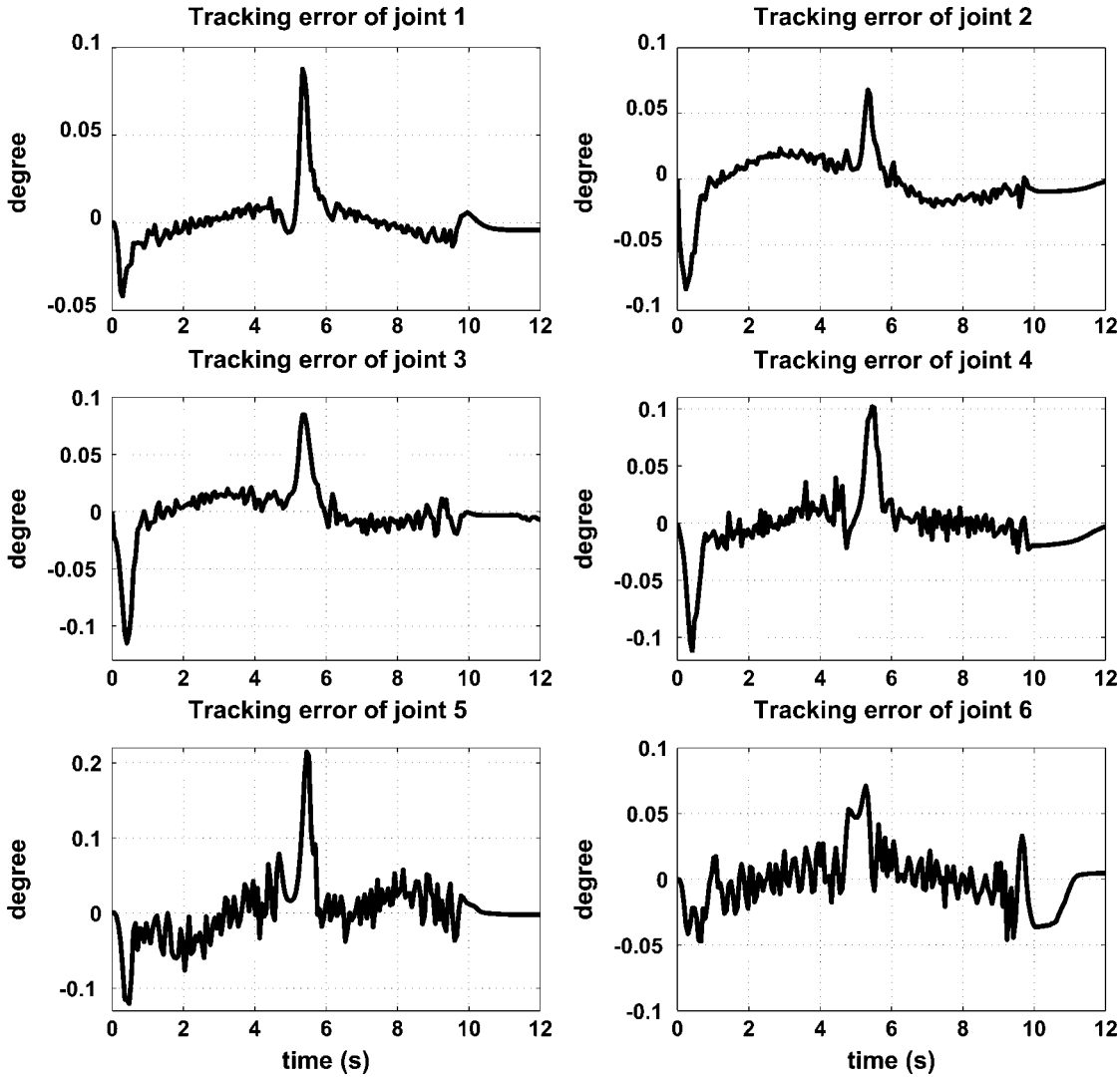

Fig. 7. Experimental results of Faraman AC2 with 4.4 kg payload under the PID control with the same PID gains (38) as the case without payload. The accuracy achieved for all joints is almost the same as the case without payload, demonstrating the robust performance of the control.

bandwidth than that of system dynamics [18], [20], [27], [34]. By Relationship 1, the proportional gain matrix $\mathbf{K}$ decreases as the sampling period L increases. That is, as the estimation error increases, $\mathbf{K}$ decreases. Generally, the robot control engineers have avoided intentionally the use of high-gain feedback in presence of large modeling estimation error (Remark 7 in [4]). Our results show that why PID gains become small under large modeling estimation error.

V. Experiments

The purpose of this experiment is to show how the PID gains are *tuned* for a real application where dynamic model including $\mathbf{g}(\mathbf{x}, \dot{\mathbf{x}})$ is *barely known* and to examine how the resulting closed-loop system performs with these gains.

The system used in the experiment is a six-DOF PUMA-type robot manipulator having maximum payload of 5 kg, Faraman AC2, made by SAMSUMG Company, as shown in Fig. 2. The DH-parameters of Faraman AC2 are listed in Fig. 3. The structure of the control system for the experiment is shown in Fig. 4. A PC was used for the main controller, and a Sensoray 626 board was used as the input/output (I/O) card. The operating system (OS) was QNX 4.2, a real-time OS, and the algorithm of the PID control was implemented in the PC.

To verify the robust performance of the PID gains, we have experimented under two different conditions: the one is without payload as illustrated in Fig. 2(a); and the other is with a payload of 4.4 kg-88% of maximum payload—as shown in Fig. 2(b). Since the change of payloads results in a significant inertia change, and more broadly in the system parameter variation, the response under it serves an excellent indication for the robust performance of the system.

Note that the same set of control gains were used for these two experiments, which was selected by using the proposed method under no-payload condition. From control designers' viewpoint, this is especially convenient, since they are free to select gains without having to pay attention to variation of payloads.

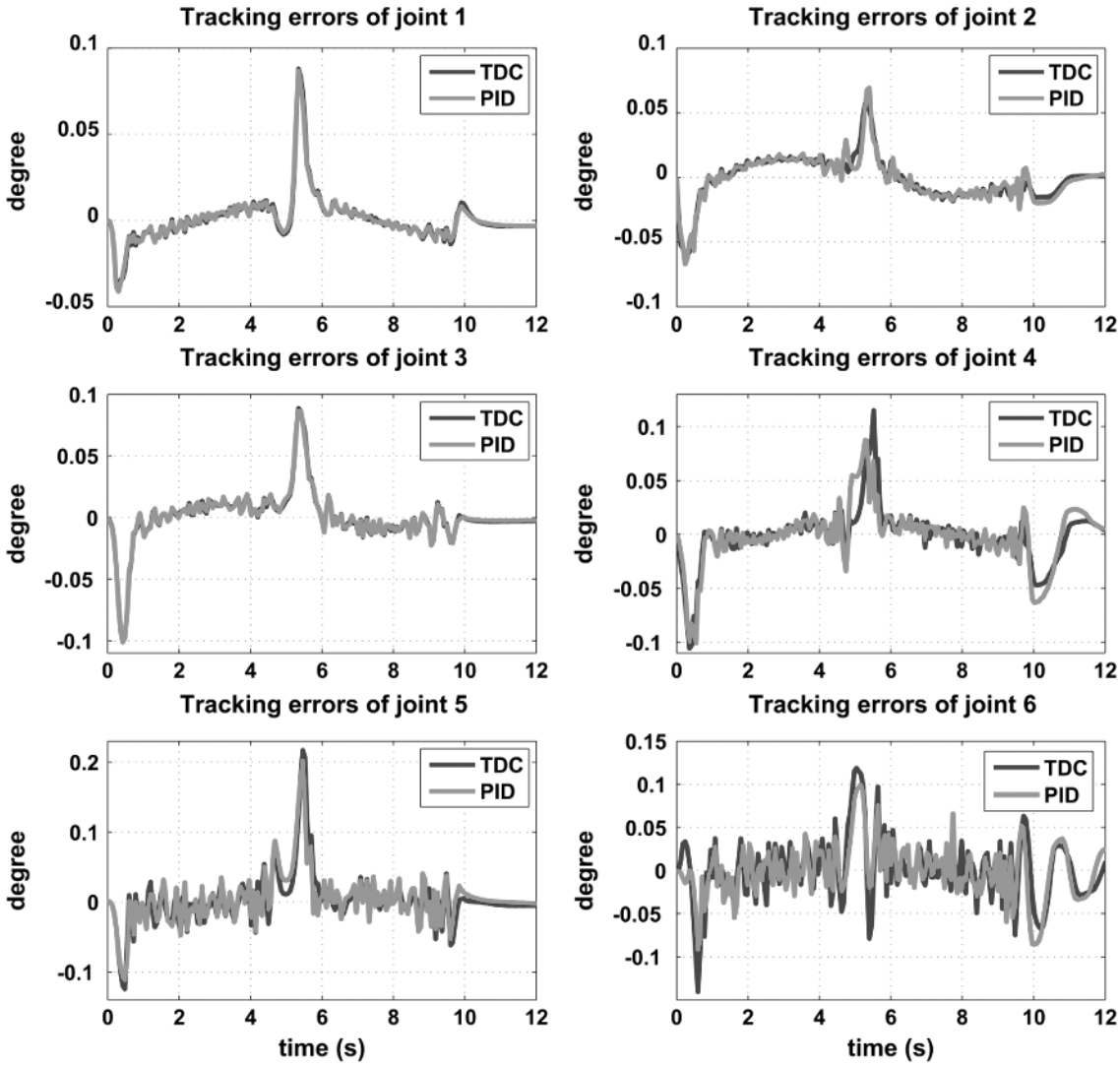

Fig. 8. Comparison of tracking error responses of the PID control with those of TDC for Faraman AC2 without payload. The responses due to the PID control are virtually identical to those of TDC, confirming the identicalness of the two.

A. *Selection of PID Gains For Faraman AC2*

A discrete PID controller for this robot manipulator is given by

$$\boldsymbol{\tau}(k) = \mathbf{K}\left(\mathbf{e}(k-1) + \mathbf{T}_D\left(\frac{\mathbf{e}(k-1)-\mathbf{e}(k-2)}{L}\right) + \mathbf{T}_I^{-1}\sum_{i=0}^{k-1} L\mathbf{e}(i)\right) + \boldsymbol{\tau}_{\mathrm{DC}} \quad (37)$$

where $\boldsymbol{\tau}(k) \in \Re^6$ denotes the torque input vector, $\mathbf{e}(k) = \boldsymbol{\theta}_d(k) - \boldsymbol{\theta}(k)$, with $\boldsymbol{\theta}_d(k) \in \Re^6$ the desired joint vector, $\boldsymbol{\theta}(k) \in \Re^6$ the real joint vector at the kth sampling instant and $\boldsymbol{\tau}_{\mathrm{DC}} \in \Re^6$ denotes the constant vector determined by (28).

The PID gain matrices $(\mathbf{K}, \mathbf{T}_D, \mathbf{T}_I)$, and $\boldsymbol{\tau}_{\mathrm{DC}}$ are determined by the proposed method as follows.

Step 1) A sampling period L is set to $L = 0.001$ s; the value of the sampling time was chosen by considering the specification of used PC and I/O card.

Step 2) For all joints, it is considered that identical desired error dynamics is achieved by $\zeta = 1$ and $\omega_n = 10$, that is, $\mathbf{k}_D = 20 \cdot \mathbf{I}_6$ and $\mathbf{k}_P = 100 \cdot \mathbf{I}_6$.

Step 3) By $\mathbf{k}_D$ and $\mathbf{k}_P$ in Step 1) and Relationship 1, $\mathbf{T}_D$ and $\mathbf{T}_I$ are obtained as

$$\mathbf{T}_D = 0.05 \cdot \mathbf{I}_6, \quad \mathbf{T}_I = 0.2 \cdot \mathbf{I}_6.$$

In determining $\bar{\mathbf{g}}$, Type II was used: $\bar{g}_1$ for the arm part and $\bar{g}_2$ for the wrist part in

$$\bar{\mathbf{g}} = \begin{bmatrix} \bar{g}_1 \cdot \mathbf{I}_3 & \mathbf{0}_3 \\ \mathbf{0}_3 & \bar{g}_2 \cdot \mathbf{I}_3 \end{bmatrix}.$$

By Relationship 1 and (28), $\mathbf{K}$ and $\boldsymbol{\tau}_{\mathrm{DC}}$ are given as

$$\mathbf{K} = 20000 \cdot \begin{bmatrix} \bar{g}_1^{-1}\mathbf{I}_3 & \mathbf{0}_3 \\ \mathbf{0}_3 & \bar{g}_2^{-1}\mathbf{I}_3 \end{bmatrix}$$

$$\boldsymbol{\tau}_{\mathrm{DC}} = \begin{bmatrix} \bar{g}_1^{-1}\mathbf{I}_3 & \mathbf{0}_3 \\ \mathbf{0}_3 & \bar{g}_2^{-1}\mathbf{I}_3 \end{bmatrix} [(\ddot{\mathbf{e}}(0) + 20 \cdot \dot{\mathbf{e}}(0)) - 1000(\dot{\mathbf{e}}(0) + 20 \cdot \mathbf{e}(0))].$$

As for desired joint trajectory, a fifth polynomial trajectory was incorporated for each joint, as shown in Fig. 5. As $\ddot{\mathbf{e}}(0) = \dot{\mathbf{e}}(0) = \mathbf{e}(0) = \mathbf{0}$ for the desired trajectory, $\boldsymbol{\tau}_{\mathrm{DC}} = \mathbf{0}$.

As was mentioned, $\alpha_1 = \bar{g}_1^{-1}$ and $\alpha_2 = \bar{g}_2^{-1}$ have been tuned in a decoupled way by trial-and-error, $\mathbf{K}$ has been determined accordingly. At first, letting α_2 be zero, α_1 is increased from very small value (0.000001) until acceptable tracking errors of joint 1–3 are obtained. The reason of starting from very small value is to avoid divergent situation of robot manipulator for the sake of safety. After finishing selection of α_1, α_2 is increased from very small value (0.000001) until acceptable tracking errors of joint 4–6 are obtained. At this moment, α_1 is set to tuned value.

The procedure was truly simple, straightforward, and fast; it took about 30 minutes to select the complete gains. The final values for α_1 and α_2 are: $\alpha_1 = 9 \times 10^{-4}$ and $\alpha_2 = 1.75 \times 10^{-4}$; and $\mathbf{K}$ was obtained as follows:

$$\mathbf{K} = \begin{bmatrix} 18 \cdot \mathbf{I}_3 & \mathbf{0}_3 \\ \mathbf{0}_3 & 3.5 \cdot \mathbf{I}_3 \end{bmatrix}.$$

Finally, 18 PID gains were determined as

$$\mathbf{K} = \begin{bmatrix} 18 \cdot \mathbf{I}_3 & \mathbf{0}_3 \\ \mathbf{0}_3 & 3.5 \cdot \mathbf{I}_3 \end{bmatrix}$$
$$\mathbf{T}_D = 0.05 \cdot \mathbf{I}_6$$
$$\mathbf{T}_I = 0.2 \cdot \mathbf{I}_6. \tag{38}$$

B. Control of Faraman AC2

The experimental results of the PID control with the gains of (38) are shown in Figs. 6 and 7: Fig. 6 shows the results under no payload condition and Fig. 7 shows the payload of 4.4 kg. Given the desired joint trajectory in Fig. 5, all the joints are to track it under the two conditions.

Fig. 6 shows the tracking errors ($\mathbf{e} = \boldsymbol{\theta}_d - \boldsymbol{\theta}$) of all the joints, the size of which are $|e_i| \leq 0.1^\circ$, for $i = 1, \ldots, 4$ and $|e_i| < 0.2^\circ$, for $i = 5, 6$. Expressing the results in terms of *% error* defined as

$$\%\ \text{error} = \frac{|e|_{\max}}{\max(\theta_d)} \times 100 \tag{39}$$

we could achieve the accuracy of 0.25% error for $i = 1, \ldots, 4$ and that of 0.5% error for $i = 5, 6$.

Fig. 7 shows experimental results with 4.4-kg payload. Clearly the sizes of errors are nearly the same as those in Fig. 6. These results show that the PID gains selected with the proposed tuning method has robust performance. This is in accordance with our reasoning and prediction in Section III that the discrete PID control shares the robust performance and simplicity with the discrete TDC because the two controls are identical. The identicalness, too, can be confirmed quantitatively by comparing the responses in Fig. 8 due to the two inputs. In Fig. 8, TDC means the response controlled by (16) with

$$\bar{\mathbf{g}} = \begin{bmatrix} (10000/9) \cdot \mathbf{I}_3 & \mathbf{0}_3 \\ \mathbf{0}_3 & (400/7) \cdot \mathbf{I}_3 \end{bmatrix}, \mathbf{k}_D = 20 \cdot \mathbf{I}_6$$

and $\mathbf{k}_P = 100 \cdot \mathbf{I}_6$ obtained from Steps 2) and 3). As was predicted in Section III, the two inputs create nearly equivalent error responses.

VI. Conclusion

This study has produced three important results: the first is a systematic method to select gains of a robust PID control applicable to *nonlinear systems*; the second is a simple and effective method for *tuning PID gains* applicable to nonlinear systems with *inaccurate models*; and the third is an *equivalence relationship* between the PID control and TDC in a discrete-time domain. These results have been made possible by relating a well proven control technique for nonlinear plants to the PID control through the finding of the equivalence relationship.

Through experiments with the industrial 6-DOF PUMA-type robot, the model of which is not well known, we have demonstrated that the proposed tuning method is simple and straightforward, yielding rapidly the PID gains. The closed-loop responses with these gains displayed adequate and robust performances.

The first and second results are especially useful for practicing control engineers who are familiar with PID control, but not familiar with (or not able to use) TDC. In addition, the tuning method will be particularly valuable in many application situations where a PID is the only control structure provided, and where users are required to tune its gains. The third result will be useful for providing valuable insights, as progress on either TDC or PID control can lead to an immediate mutual benefit.

References

[1] Y. Lin, K. H. Ang, and G. C. Y. Chong, "Patents, software, and hardware for PID control," *IEEE Control Syst. Mag.*, vol. 26, no. 1, pp. 42–54, Feb. 2006.

[2] *PID 2006, IEEE Contr. Syst. Mag.*, vol. 26, no. 1, Feb. 2006.

[3] W. Li, X. G. Chang, F. M. Wahl, and J. Farrell, "Tracking control of a manipulator under uncertainty by fuzzy P+ID controller," *Fuzzy Sets Syst.*, vol. 122, no. 1, pp. 125–137, 2001.

[4] I. Cervantes and J. Alvarez-Ramirez, "On the PID tracking control of robot manipulators," *Syst. Control Lett.*, vol. 42, no. 1, pp. 37–46, 2001.

[5] H. B. Kazemian, "The SOF-PID controller for the control of a MIMO robot arm," *IEEE Trans. Fuzzy Syst.*, vol. 10, no. 4, pp. 523–532, Apr. 2002.

[6] W. Li, X. G. Chang, J. Farrell, and F. M. Wahl, "Design of an enhanced hybrid fuzzy P+ID controller for a mechanical manipulator," *IEEE Trans. Syst., Man, Cybern. B, Cybern.*, vol. 31, no. 6, pp. 938–945, Dec. 2001.

[7] Y. L. Sun and M. J. Er, "Hybrid fuzzy control of robotics systems," *IEEE Trans. Fuzzy Syst.*, vol. 12, no. 6, pp. 755–765, Dec. 2004.

[8] S. Yildirim, M. F. Sukkar, R. Demirci, and V. Aslantas, "Design of adaptive NNs-robust-PID controller for a robot control," in *Proc. IEEE Int. Symp. Intell. Control*, Dearborn, MI, 1996, pp. 508–513.

[9] D. P. Kwok and F. Sheng, "Genetic algorithm and simulated annealing for optimal robot arm PID control," in *Proc. 1st IEEE Conf. Evolutionary Computation*, Orlando, FL, 1994, pp. 707–713.

[10] J. Park and W. K. Chung, "Analytic nonlinear H_∞ inverse-optimal control for euler-lagrange system," *IEEE Trans. Robot. Autom.*, vol. 16, no. 6, pp. 847–854, Dec. 2000.

[11] Y. Choi and W. K. Chung, "Performance limitation and autotuning of inverse optimal PID controller for lagrangian systems," *ASME J. Dynam. Syst. Meas. Control*, vol. 127, no. 2, pp. 240–248, 2005.

[12] J. Park and W. Chung, "Design of a robust H_∞ PID control for industrial manipulators," *ASME J. Dynam. Syst. Meas. Control*, vol. 122, no. 4, pp. 803–812, 2000.

[13] E. Eriksson and J. Wikander, "Robust PID design of flexible manipulators through pole assignment," in *Proc. 7th Int. Workshop Adv. Motion Control*, Maribor, Slovenia, 2002, pp. 420–425.

[14] J. Alvarez-Ramirez, I. Cervantes, and R. Bautista, "Robust PID control for robots manipulators with elastic joints," in *Proc. IEEE Int. Conf. Control Appl.*, Mexico City, Mexico, 2001, pp. 542–547.

[15] K. J. Åström and T. Hägglund, *Automatic Tuning of PID Controls*. Triangle Park, NC: Instrument Society of America, 1988.

[16] G. P. Liu and S. Daley, "Optimal-tuning PID control for industrial systems," *Control Eng. Pract.*, vol. 9, no. 11, pp. 1185–1194, 2001.

[17] G. F. Franklin, J. D. Powell, and A. Emami-Naeini, *Feedback Control of Dynamic Systems*, 3rd ed. Boston, MA: Addison-Wesley, 1994.

[18] K. Youcef-Toumi and O. Ito, "A time delay controller for systems with unknown dynamics," *ASME, J. Dynam. Syst. Meas. Control*, vol. 112, no. 1, pp. 133–142, 1990.

[19] K. Youcef-Toumi and S.-T. Wu, "Input/output linearization using time delay control," *ASME, J. Dynam. Syst. Meas. Control*, vol. 114, no. 2, pp. 10–19, 1992.

[20] T. C. Steve Hsia, "A new technique for robust control of servo systems," *IEEE Trans. Ind. Electron.*, vol. 36, no. 1, pp. 1–7, Feb. 1989.

[21] T. C. Steve Hsia, T. A. Lasky, and Z. Guo, "Robust independent joint controller design for industrial robot manipulators," *IEEE Trans. Ind. Electron.*, vol. 38, no. 1, pp. 21–25, Feb. 1991.

[22] K. Youcef-Toumi and C. C. Shortlidge, "Control of robot manipulator using time delay," in *Proc. IEEE Int. Conf. Robot. Autom.*, Sacramento, CA, 1991, pp. 2391–2395.

[23] T. C. Hsia and L. S. Gao, "Robot manipulator control using decentralized linear time-invariant time-delayed joint controllers," in *Proc. IEEE Int. Conf. Robot. Autom.*, OH, 1990, pp. 2070–2075.

[24] S. Jung, T. C. Hsia, and R. G. Bonitz, "Force tracking impedance control of robot manipulators under unknown environment," *IEEE Trans. Control Syst. Technol.*, vol. 12, no. 3, pp. 474–483, May 2004.

[25] P. H. Chang, B. S. Park, and K. C. Park, "An experimental study on improving hybrid position/force control of a robot using time delay control," *Mechatron.*, vol. 6, no. 8, pp. 915–931, 1996.

[26] K. Youcef-Toumi and S. Reddy, "Dynamic analysis and control of high speed and high precision active magnetic bearing," *ASME J. Dynam. Syst. Meas. Control*, vol. 114, no. 4, pp. 623–632, 1992.

[27] P. H. Chang, S. H. Park, and J. H. Lee, "A reduced order time delay control highly simplified brushless DC motor," *ASME J. Dynam. Syst. Meas. Control*, vol. 121, no. 3, pp. 556–560, 1999.

[28] P. H. Chang and S. J. Lee, "A straight-line motion tracking control of hydraulic excavator system," *Int. J. Mechatron.*, vol. 12, no. 1, pp. 119–138, 2002.

[29] P. H. Chang and S. U. Lee, "Control of a heavy-duty robotic excavator using time delay control with integral sliding surface," *Control Eng. Pract.*, vol. 10, no. 7, pp. 697–711, 2002.

[30] J. Y. Park and P. H. Chang, "Vibration control of a telescopic handler using time delay control and a commandless input shaping technique," *Control Eng. Pract.*, vol. 12, no. 6, pp. 769–780, 2004.

[31] H. S. Jeong and C. W. Lee, "Time delay control with state feedback for azimuth motion of the frictionless positioning device," *IEEE Trans. Mechatron.*, vol. 2, no. 3, pp. 161–168, Jun. 1997.

[32] K.-H. Kim and M.-J. Youn, "A simple and robust digital current control technique of a PM synchronous motor using time delay control approach," *IEEE Trans. Power Electron.*, vol. 16, no. 1, pp. 72–81, Jan. 2001.

[33] J. H. Jung, P.-H. Chang, and O.-S. Kwon, "A new stability analysis of time delay control for input/output linearizable plants," in *Proc. Amer. Control Conf.*, Boston, MA, 2004, pp. 4972–4979.

[34] P. H. Chang and S. H. Park, "On improving time-delay control under certain hard nonlinearities," *Mechatron.*, vol. 13, no. 4, pp. 393–412, 2003.

[35] G. R. Cho, P. H. Chang, and S. H. Park, "Robust trajectory control of robot manipulators using time delay estimation and internal model concept," in *Proc. 44th IEEE Conf. Decision Control Eur. Control Conf.*, Seville, Spain, 2005, pp. 3199–3206.

[36] C. J. Li, "A new method of dynamics for robot manipulators," *IEEE Trans. Syst. Man Cybern.*, vol. 18, no. 1, pp. 105–114, Jan./Feb. 1988.